Available online at www.sciencedirect.com

SciVerse ScienceDirect

Physics Procedia 31 (2012) 147 – 157

Physics Procedia

GAMMA-1 Emission of Prompt Fission Gamma-Rays in Fission and Related Topics

Global view on fission observables - new insights and new puzzles

Karl-Heinz Schmidt[a]*, Beatriz Jurado

CENBG, CNRS/IN2P3, Chemin du Solarium, B.P. 120, 33175 Gradignan, France

Abstract

An overview is given on some measurable quantities that carry information on the evolution of the fissioning system from the quasi-bound configuration to the final fission fragments in their respective ground states. New insights into the nature of the fission process, but also new puzzles, emerging from recent experimental findings, are presented. They cover the following topics:
Dynamics: Early freeze-out due to dynamical effects; importance of quantum-mechanical effects for fluctuations and angular-momentum pumping.
Systematics of fission channels: Separability principle, a powerful application of the macroscopic-microscopic approach to fission; the puzzle of the apparent role of proton shells.
Energetics: Transformation of the potential-energy gain into kinetic energy, single-particle excitations, and collective excitations; heat transfer between the nascent fragments; consequences for prompt-neutron emission and the even-odd effect in fragment yields; ambiguities and model dependences.

New experimental knowledge on the nuclear level density is included in the discussion.

Keywords: Fission channels; prompt-neutron yields; even-odd effect; semi-empirical model; energy sorting

[a]* Corresponding author. Tel.: +49-6150-82314
E-mail address: schmidt-erzhausen@t-online.de

doi:10.1016/j.phpro.2012.04.020

1. Introduction

Since the discovery of nuclear fission by Hahn and Straßmann in 1939 [1], the progress in the understanding of this dramatic nuclear re-organization process has not ceased being stimulated by new experimental findings. Although the gross explanation of nuclear fission on the basis of the liquid- drop model was provided very soon by Bohr and Wheeler [2], new observations permanently revealed a more and more detailed view on the complexity of nuclear fission and created new challenges for theory. Research on nuclear fission, in particular low-energy fission, where the influence of nuclear structure is strong, also yielded profit for the understanding of nuclear properties in general. The observation of asymmetric fission promoted the development of the nuclear shell model [3,4]. The existence of shape isomers proved that shell effects persist at large deformations [5]. In the 1980's, a rather comprehensive understanding of the fission process had seemed to be reached, which is documented in the well-known book of Wagemans [6]. Among the most important achievements were the development of the concept of fission channels [7] and the study of the even-odd effect in fission-fragment Z distributions [8,9]. But new discoveries in the domain of nuclear fission are emerging continuously up to present times. The present contribution deals with some new theoretical ideas, which solve long-standing problems, and a few very recent findings, which represent new puzzles to theory.

2. Experimental methods

2.1. Available fissioning nuclei

The progress in the understanding of fission heavily relied and still relies on the development of advanced experimental methods. A severe restriction is still the availability of fissionable material as target material. Therefore, the traditional use of neutrons for inducing fission offers only a rather limited choice of fissioning systems. These limitations were more and more overcome by alternative methods: Spontaneously fissioning heavy nuclei were produced by fusion reactions [10]. Exotic nuclei were produced in spallation reactions which undergo beta-delayed fission [11]. Electromagnetic-induced fission of neutron-deficient radioactive nuclei, produced as projectile fragments from a ^{238}U primary beam, was studied in-flight at relativistic energies [12]. Very recently, comprehensive studies on fission of transfer products of ^{238}U projectiles have been performed [13].

2.2 Detection and resolution

The identification of the fission products poses a severe problem. First experiments, which were based on radiochemical methods [14], were not fast enough to determine the yields of short-lived fragments and suffered from normalization problems. Kinematic identification methods by double time-of-flight [15,16] and double-energy measurements [17] provided full mass distributions, however with limited resolution. The LOHENGRIN spectrograph brought big progress in identifying the nuclear charges of the light fission products [18]. However, full isotopic identification (in Z and A) of the fission products has only been achieved by boosting the energies of the products in inverse-kinematics experiments and using powerful magnetic spectrometers [12,13,19].

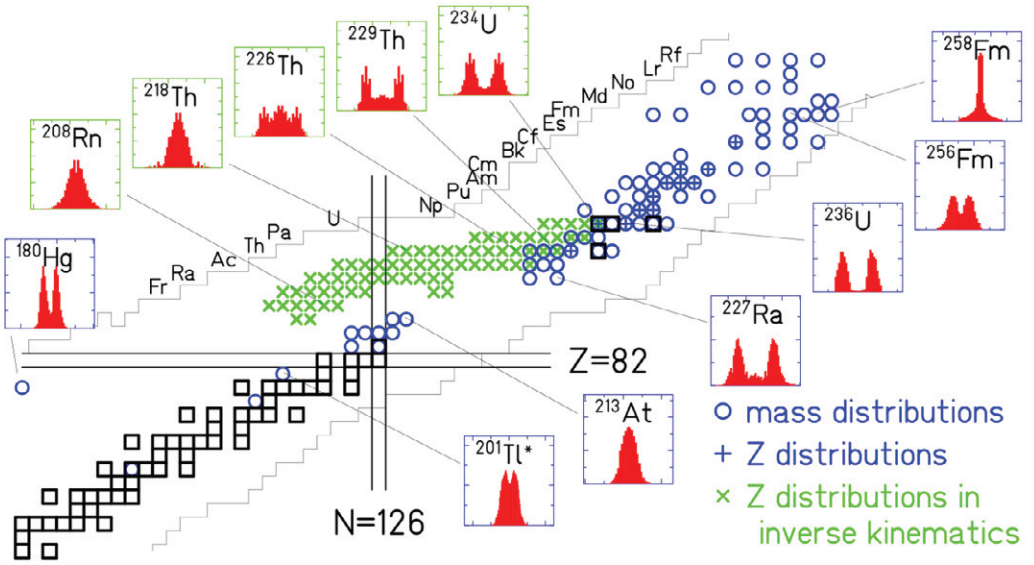

Figure 1: General view on the systems for which mass or nuclear-charge distributions have been measured. The distributions are shown for 12 selected systems. Blue circles (blue crosses): Mass (nuclear-charge) distributions, measured in conventional experiments [11,20] and references given in [12]. Green crosses: Nuclear-charge distributions, measured in inverse kinematics [12].

3. Fission channels

3.1 Experimental systematics

Figure 1 gives an overview on the measured mass and nuclear-charge distributions of fission products from low-energy fission. Fission of target nuclei in the actinide region, mostly induced by neutrons, shows predominantly asymmetric mass splits. A transition to symmetric mass splits is seen around mass 258 in spontaneous fission of fusion residues. Electromagnetic-induced fission of relativistic secondary beams covers the transition from asymmetric to symmetric fission around mass 226. A pronounced fine structure close to symmetry appears in ^{201}Tl [20] and in ^{180}Hg [11]. It is difficult to observe low-energy fission in this mass range. Thus, ^{201}Tl could only be measured down to 7.3 MeV above the fission barrier due to its low fissility, which explains the filling of the minimum between the two peaks. Only ^{180}Hg was measured at energies close to the barrier after beta decay of ^{180}Tl. Considering the measured energy-dependence of the structure for ^{201}Tl [20], the fission characteristics of these two nuclei are rather similar. Also other nuclei in this mass region show similar features [21].

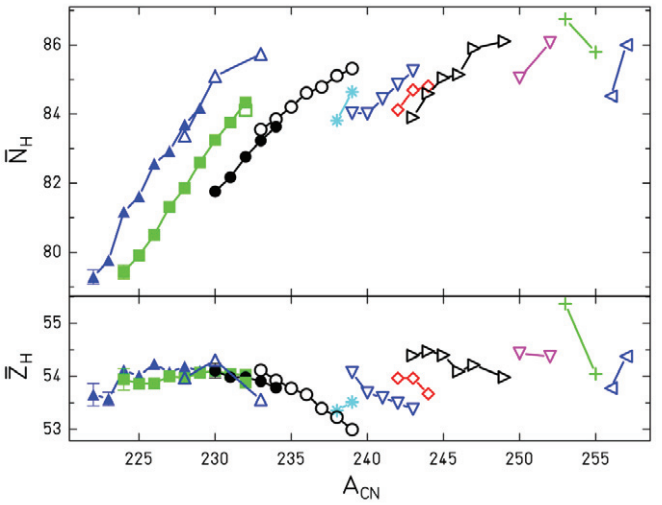

Figure 2: Mean neutron and proton number of the heavy component in asymmetric fission in the actinide region. The values were deduced from measured mass and nuclear-charge distributions using the semi-empirical GEF code [24] for the correction of charge polarization and prompt-neutron emission. Open symbols denote results from conventional experiments; full symbols refer to an experiment with relativistic projectile fragments of ^{238}U [12] (See [24] for references of the underlying experimental data).

3.2 Size of the heavy fragment in asymmetric fission

In the range where asymmetric fission prevails, e.g. from ^{227}Ra to ^{256}Fm, the light and the heavy fission-product components gradually approach each other, see figure 1. A quantitative analysis reveals that the mean mass of the heavy component stays approximately constant [22] at about $A = 140$. This has been explained by the influence of a deformed ($\beta \approx 0.6$) fragment shell at $N = 88$ and the spherical shell at $N = 82$ [23], suggesting that the position of the heavy fragment is essentially constant in neutron number.

New data on Z distributions over long isotopic chains [12], however, reveal very clearly that the position in neutron number varies systematically over more than 7 units, while the position in proton number is approximately constant at $Z = 54$, see Fig. 2. The rather short isotopic sequences covered in former experiments did not allow deducing this feature and gave the false impression of a constant position in mass. This finding represents a severe puzzle to theory, since shell-model calculations do not show any shell stabilization near $Z = 54$ at $\beta \approx 0.6$ [23,25].

3.3 Separability principle

The microscopic-macroscopic approach has proven to be very useful for calculating nuclear properties, in particular in applications to fission [26]. The early influence of fragment shells on the fission path, deduced from two-centre shell-model calculations [27], makes its application to fission even more powerful. It means that the microscopic properties of the fission observables are essentially determined by the shells of the fragments, and only the macroscopic properties are specific to the fissioning system [28].

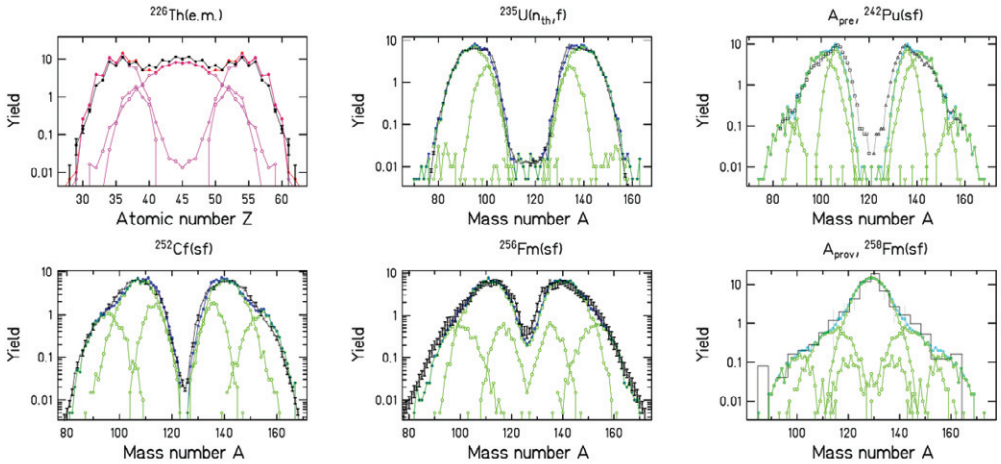

Figure 3: Nuclear-charge and post-neutron mass distributions of fission fragments (For ^{258}Fm(sf) the "provisional mass" A_{prov} is shown, which is directly deduced from the ratio of the kinetic energies of the fragments and, thus, not corrected for neutron emission). Experimental data (black lines, respectively histogram) for electromagnetic-induced (e.m.), thermal-neutron-induced (n_{th},f) and spontaneous fission (sf) are compared with predictions of the GEF code [24] (red and green lines). The contributions of different fission channels are shown. (see [24] for references of the data).

This "separability principle" was exploited in the GEF code [24], which relies on an empirical description of the macroscopic stiffness parameters in the relevant normal modes and empirically deduced fragment shells, which are valid for all fissioning systems. Figure 3 demonstrates that the mass distributions over a large range of systems can be described very well with the same parameter set.

3.4 Dynamical effects

Statistical scission-point models, e.g. ref. [23], suffer from the neglect of dynamical effects. Stochastic calculations revealed that, depending on the nature of the collective degree of freedom, dynamical effects induce a kind of memory on the fission trajectory, which may be accounted for by an early freeze-out that depends on the influence of inertia. Mass-asymmetric distortions have a large inertia, and thus the mass distribution is already essentially determined slightly behind the outer fission saddle [29]. Charge polarization has a small inertia, and the distribution is determined close to scission [30].

3.5 Fluctuations

Most fission observables form bell-shaped distributions around a mean value. This suggests treating the corresponding collective degree of freedom as an harmonic quantum oscillator coupled to a heat bath of temperature T. Especially for the charge-polarization degree of freedom there is a long discussion about the importance of the zero-point motion [31,32]. Nix estimated the level spacing in the oscillator corresponding to mass-asymmetric distortions at saddle with the liquid-drop model to 1-2 MeV in the actinide region [33]. According to the smaller widths of the corresponding components to the mass

distribution, the level spacing for oscillations in the two asymmetric fission valleys (Standard 2 and Standard 1) is about 5 and more than 10 MeV, respectively. Also for oscillations in the charge-polarization degree of freedom, the level spacing is in the order of 10 MeV. These values are appreciably larger than the temperature values of actinides, which are about 0.5 MeV in the constant-temperature regime [34]. Thus, in a statistical approach these degrees of freedom are essentially not excited, and the widths of the corresponding distributions are essentially determined by the zero-point motion.

Also the angular-momentum distributions of the fragments have been explained by "orientation pumping" due to the uncertainty principle [35]. Experimental indications for thermal excitations of spherical fragments [36] have also been explained by the compensation of the orbital angular momentum, which itself is induced by the zero-point motion [37]. Here it is the operator of the orbital angular momentum which does not commute with the angle that characterizes the direction of particle motion. Thus, all fragment angular momenta measured in low-energy fission are explained by the quantum-mechanical uncertainty principle. There is no room for excitations of the angular-momentum-bearing modes [38].

Due to the strong influence of quantum-mechanical effects it is mandatory to explicitly consider quantum-mechanical effects, as it is e.g. done in the self-consistent microscopic approach of Ref. [39]. Stochastic approaches with classical models [40] seem to be inadequate.

4. Prompt-neutron yields

4.1 Transformation of energy – the different contributions

In low-energy fission, the Q value of the reaction ends up either in the total kinetic energy (TKE) or the total excitation energy (TXE) of the fragments. The TKE is closely related to the distance of the centers of the two nascent fragments at scission, but it cannot give information on the shapes of the individual fragments. The TXE, however, can be attributed to the individual fragments by a kinematical measurement of the prompt-neutrons. Still, there is no direct experimental information on the processes, which are responsible for the transformation of part of the Q value into the excitation energies of the separated fragments. The situation is schematically illustrated in Fig. 4. Before scission, dissipation leads to intrinsic excitations, collective modes perpendicular to the fission direction ("normal modes" [33]) may be excited, and, finally, some energy is stored in deformation of the nascent fragments that is induced by the Coulomb repulsion. The remaining part is found as pre-scission kinetic energy [41]. After scission, collective excitations and deformation energy are transformed and add up to the intrinsic excitations of the separated fragments. The situation at scission is important for the understanding of fission dynamics, e.g. the magnitude of dissipation and the coupling between the different collective degrees of freedom, but without additional information, the repartition remains ambiguous.

4.2 Origin of the saw-tooth shape

There is widespread agreement that the saw-tooth shape of the prompt-neutron yields, see figure 5, is caused by the deformation energies of the nascent fragments at scission. The scission-point model of ref.

[23] attributes it to the influence of fragment shells, the random-neck-rupture model [7] links it to the location of the rupture, and also microscopic calculations predict large deformation energies of the fragments near scission [42]. Large even-odd effects in the fragment Z distributions indicate that the intrinsic excitation energy at scission is generally much too low to account for the variation of the prompt-neutron yield by several units over the different fragments.

4.3 Differential behavior – energy sorting

Recent experimental results reveal that nuclei exhibit an essentially constant temperature up to excitation energies of 20 MeV [44] with a temperature parameter, which is grossly proportional to $A^{-2/3}$ [34]. This behavior is explained by the breaking of pairs in the so-called superfluid regime [45]. This leads to a considerable increase of the heat capacity [46] and consequently to a slow variation of temperature as a function of excitation energy. Note that the BCS approximation severely underestimates the pairing condensation energy and consequently also the magnitude of the heat capacity in the so-called superfluid regime [47]. Thus the assumption of a constant nuclear temperature becomes a good approximation. This implies that the intrinsic excitation energy of the two nascent fragments at scission is subject to energy sorting [48,49,50]: The hotter light fragment transfers essentially all its intrinsic excitation energy to the colder heavy fragment. This energy sorting manifests itself in the mass-dependent neutron yields. Figure 5 shows data for neutron-induced fission of ^{237}Np with E_n = 0.8 MeV and E_n = 5.55 MeV as an example. The additional initial energy leads to an increased neutron yield from the heavy fragments, only. The behavior is well reproduced by the GEF code, which includes a model for the process of energy sorting.

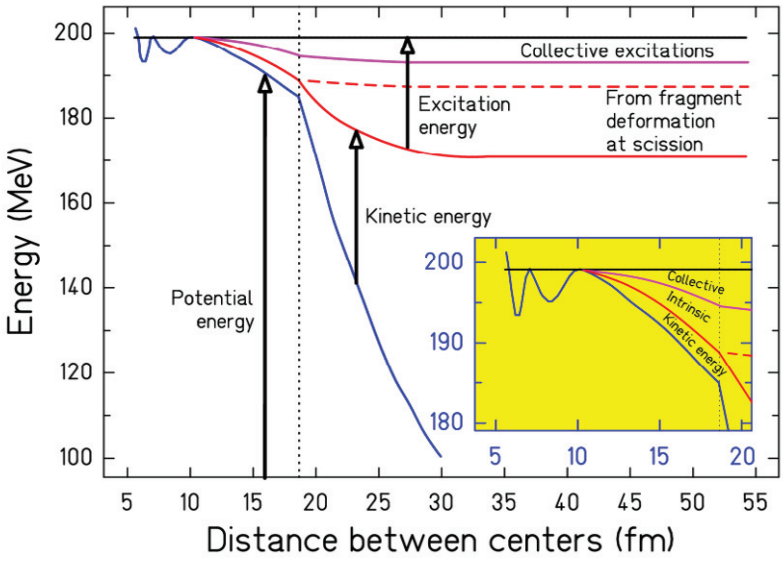

Figure 4: Schematic drawing of the transformation of energy during the fission process of ^{236}U with an initial excitation energy equal to the height of the fission barrier.

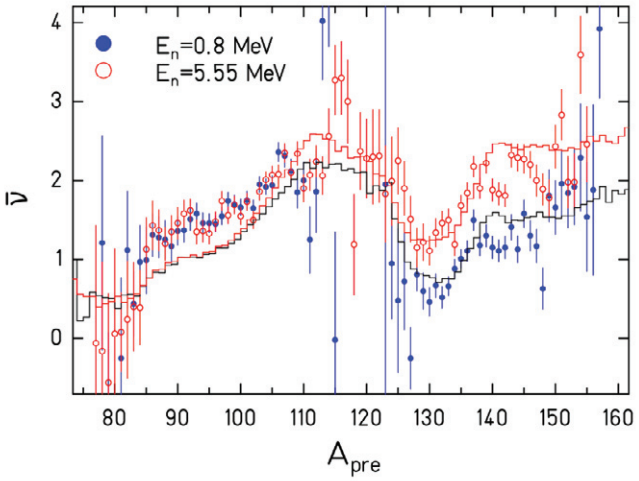

Figure 5: Measured prompt-neutron yield in ^{237}Np(n,f) as a function of pre-neutron mass at two different incident-neutron energies [43] (data points) in comparison with the result of the GEF code [24] (histograms).

5. Even-odd effect

5.1 Experimental systematics

A systematic view on the local even-odd effect in fission-fragment *Z* distributions [51] reveals a regular pattern and a general dependence on the fissioning system, see Fig. 6. The magnitude of the even-odd effect is small at symmetry, and it increases strongly with increasing asymmetry. At the same time, the even-odd effect generally decreases for heavier systems. The even-odd effect in the light fragment group of even-*Z* and odd-*Z* systems is essentially identical, except at symmetry, where the even-odd effect in odd-*Z* systems is exactly zero. Electromagnetic excitations lead to slightly higher excitation energies, thus reducing the magnitude of the even-odd effect. The large number of systems investigated revealed that the appearance of a large even-odd effect at large asymmetry is a general phenomenon, also in odd-*Z* fissioning systems [52]. In any case, there is an enhancement for even-*Z* fragments in the light fragment group, indicating that it is the enhanced production of even-*Z* light fragments in their ground state, which is at the origin of the large even-odd effect at extreme asymmetry.

5.2 Final stage of energy sorting

It seems straightforward to attribute the enhanced production of even-Z light fragments to the energy-sorting mechanism [53] that explained already the differential behaviour of the prompt-neutron yields. If the time until scission is sufficient for the energy sorting to be accomplished, the system can still gain an additional amount of entropy by predominantly producing even-even light fragments. Compared to the production of odd-odd light fragments, the excitation energy of the heavy fragment increases by two times the pairing gap, and its entropy increases due to the increasing number of available states. The right

part of figure 6 shows a calculation with the GEF code, where this idea is included in a schematic way. The basic features are: (i) The excitation energy induced by dissipation grows with the Coulomb parameter $Z^2/A^{1/3}$, and the time needed for complete energy sorting is correspondingly increased. This explains the observed reduction of the even-odd effect for heavier systems. (ii) The thermal pressure grows with increasing asymmetry, which accelerates the energy-sorting process. This explains the strong increase of the even-odd effect at large asymmetry.

The asymmetry-driven even-odd effect is thus a threshold phenomenon, which sets in when the time needed for reaching the scission configuration is sufficiently long for complete energy sorting. Fluctuations in the energy-sorting process are responsible for the smooth onset of the even-odd effect with increasing asymmetry.

6. Summary

New approaches extended the availability of fissioning systems for experimental studies on low-energy fission considerably and provided a full identification of all fission products in A and Z for the first time. The systematics of available data gives a more comprehensive view on the influence of shell effects and pairing correlations on the fission-fragment mass and nuclear-charge distributions. The previously claimed constant mean mass of the heavy component in asymmetric fission turned out to be biased by the restricted empirical knowledge. New data reveal that it is the position of the heavy component in Z, which is approximately constant. Theoretical arguments for this unexpected finding are not yet available.

The modelling of the fission process with dynamical models is still very difficult, since most advanced models in nuclear physics that have been developed for stationary states are not readily applicable to the decay of a meta-stable state. In addition, these models suffer from their tremendous demand on computing power, restricting severely the number of degrees of freedom to be investigated. Since quantum-mechanical effects are essential, stochastic approaches with classical models seem to be inadequate. Semi-empirical methods exploiting powerful theoretical ideas like (i) the separability of the influences of fragment shells and macroscopic influences of the compound nucleus, (ii) the properties of a quantum oscillator coupled to the heat bath of the other nuclear degrees of freedom for describing the fluctuations of normal collective modes, and (iii) an early freeze-out of collective motion to include dynamical effects seem to give a good description of the observed general trends.

The transformation of part of the fission Q value into intrinsic excitation energy along the fission process, following the laws of statistical mechanics, is essential for explaining the observed features of prompt-neutron emission and the even-odd effect in fission-fragment element yields. The threshold behaviour of the asymmetry-associated even-odd effect establishes a relation between the speed of the energy transfer between the nascent fragments and the dynamical time, starting at the moment when the two fragments develop their individual properties, e.g. their final temperatures, and the moment when the resistance against the transfer of protons across the neck becomes inhibitive. This new insight stresses the importance of nuclear fission as a laboratory for studying the dynamics of non-equilibrium processes in mesoscopic objects under the influence of residual interactions. The relevance for the description of prompt-neutron and prompt-gamma emission is obvious.

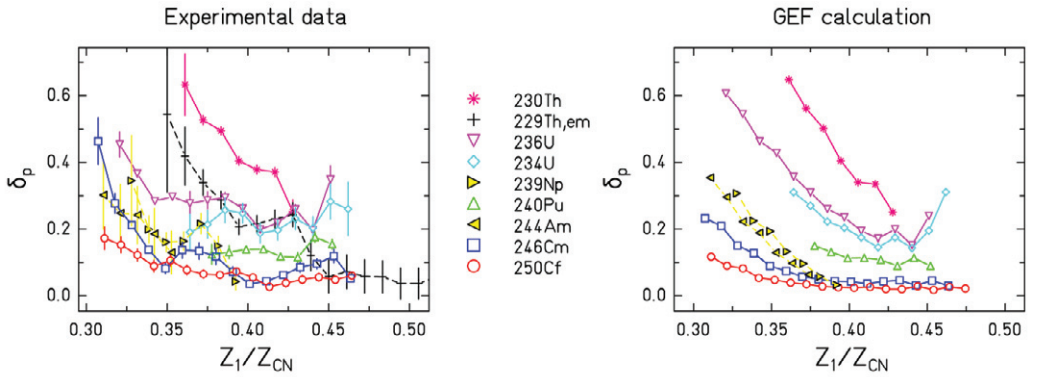

Figure 6: Measured (left) and calculated (right) local even-odd effect in fission-fragment Z distributions in (n_{th},f) reactions. The fissioning nuclei are indicated. Data for fission of ^{229}Th, induced by electromagnetic excitations are included. See ref. [51] for references of the data.

Acknowledgements

Parts of this work have been supported by the EFNUDAT network and by the ERINDA network of EURATOM. K.-H. S. thanks the CENBG for warm hospitality.

References

[1] Otto Hahn, Fritz Straßmann, Naturwissenschaften 27 (1939) 89.
[2] N. Bohr, J. A. Wheeler, Phys. Rev. 56 (1939) 426.
[3] M. Goeppert-Mayer, Phys. Rev. 74 (1948) 235.
[4] O. Haxel, J. H. D. Jensen, H. E. Suess, Phys. Rev. 75 (1949) 1766.
[5] S. G. Nilsson, Kgl. Danske Videnskab. Selskab, Mat.-Fys. Medd. 29 (1955) 16.
[6] Nuclear Fission Process, C. Wagemans ed., CRC Press Inc., (1991) .
[7] U. Brosa, S. Grossmann, A. Müller, Phys. Rep. 197 (1990) 167.
[8] H. Nifenecker et al., Z. Phys. A 308 (1982) 39.
[9] J. P. Bocquet, R. Brissot, Nucl. Phys. A 502 (1989) 213c.
[10] A. Ghiorso, T. Sikkeland, M. J. Nurmia, Phys. Rev. Lett. 18 (1967) 401.
[11] A. N. Andreyev et al., Phys. Rev. Lett. 105, 252502 (2010).
[12] K.-H. Schmidt et al., Nucl. Phys. A 665 (2000) 221.
[13] F. Farget, private communication (2011).
[14] E. A. C. Crough, At. Data and Nucl. Data Tables 19 (1977) 419.
[15] W. E. Stein, Phys. Rev. 108 (1957) 94.
[16] J. C. D. Milton and J. S. Fraser, Phys. Rev. 111 (1958) 877.
[17] H. W. Schmitt, W. E. Kiker, C. W. Williams, Phys. Rev. 137 (1965) B837.
[18] E. Moll et al., Nucl. Instrum. Methods 123 (1975) 615.
[19] C. Donzaud et al., Eur. Phys. J. A 1 (1998) 407.
[20] M. G. Itkis et al., Sov. J. Nucl. Phys. 52 (1990) 601.
[21] S. I. Mulgin, K.-H. Schmidt, A. Grewe, S. V. Zhdanov, Nucl. Phys. A 640 (1998) 375.
[22] J. P. Unik et al., Proc. Symp. Phys. Chem. Fission, Rochester 1973, IAEA Vienna (1974), vol. 2, p. 19.

[23] B. D. Wilkins, E. P. Steinberg, R. R. Chasman, Phys. Rev. C 14 (1976) 1832.
[24] http://www.cenbg.in2p3.fr/GEF.
[25] I. Ragnarsson, R. K. Sheline, Phys. Scr. 29 (1984) 385.
[26] M. Brack et al., Rev. Mod. Phys. 44 (1972) 320.
[27] U. Mosel, H. Schmitt, Phys. Rev. C 4 (1971) 2185.
[28] K.-H. Schmidt, A. Kelic, M. V. Ricciardi, Europh. Lett. 83 (2008) 32001.
[29] A. V. Karpov, P. N. Nadtochy, D. V. Vanin, G. D. Adeev, Phys. Rev. C 63, 054610 (2001).
[30] A. V. Karpov, G. D. Adeev, Eur. Phys. J. A 14 (2002) 169.
[31] H. Nifenecker, J. Physique Lett. 41 (1980) 47.
[32] B. Bouzid et al., J. Phys. G: Nucl. Part. Phys. 24 (1998) 1029.
[33] J. R. Nix, Ann. Phys. 41 (1967) 52.
[34] D. Bucurescu, T. von Egidy, Phys. Rev. C 72, 06730 (2005).
[35] L. Bonneau, P. Quentin, I. N. Mikhailov, Phys. Rev. C 75, 064313 (2007).
[36] F. Gönnenwein, I. Tsekhanovich, V. Rubchenya, Intern. J. Mod. Phys. E 16 (2007) 410.
[37] S. G. Kadmensky, Phys. Atom. Nuclei 71 (2008) 1193.
[38] L. G. Moretto, G. F. Peaslee, G. J. Wozniak, Nucl. Phys. A 502 (1989) 453c.
[39] H. Goutte, J. F. Berger, P. Casoli, D. Gogny, Phys. Rev. C 71, 024316 (2005).
[40] J. Randrup, P. Möller, A. J. Sierk, Phys. Rev. C 84, 034613 (2011).
[41] V. M. Kolomietz, S. Åberg, S. V. Radionov , Phys. Rev. C 77, 014305 (2008).
[42] N. Dubray, H. Goutte, J.-P. Delaroche, Phys. Rev. C 77, 014310 (2008).
[43] A. A. Naqvi, F. Käppeler, F. Dickmann, R. Müller, Phys. Rev. C 34 (1986) 21.
[44] A. V. Voinov et al., Phys. Rev. C 79, 031301 (2009).
[45] M. Guttormsen et al., Phys. Rev. C 68, 034311 (2003).
[46] Y. Alhassid, G. F. Bertsch, L. Fang, Phys. Rev. C 68, 044322 (2003).
[47] G. G. Dussel, S. Pittel, J. Dukelsky, P. Sarriguren , Phys. Rev. C 76, 011302 (2007).
[48] K.-H. Schmidt, B. Jurado, Phys. Rev. Lett. 104, 21250 (2010).
[49] K.-H. Schmidt, B. Jurado, Phys. Rev. C 82, 014607 (2011).
[50] K.-H. Schmidt, B. Jurado, Phys. Rev. C 83, 061601 (2011).
[51] M. Caamano, F. Rejmund, K.-H. Schmidt, J. Phys. G: Nucl. Part. Phys. 38 (2011) 035101.
[52] S. Steinhäuser et al., Nucl. Phys. A 634 (1998) 89.
[53] K.-H. Schmidt. B. Jurado, arXiv:1007.0741v1[nucl-th] (2010).